



Efficient photocatalytic degradation of toxic dyes using nanostructured TiO₂/polyaniline nanocomposite

Lalitha Gnanasekaran^a, R. Hemamalini^{a,*}, Mu Naushad^{b,*}

^aDepartment of Physics, Queen Mary's College, Chennai 600 004, India, email: hemaphy.qmc@gmail.com (R. Hemamalini)

^bDepartment of Chemistry, College of Science, Building #5, King Saud University, Riyadh, Saudi Arabia, email: shad81@rediffmail.com (M. Naushad)

Received 3 January 2018; Accepted 28 January 2018

ABSTRACT

In this study, the synergistic effect between polyaniline and TiO₂ nanoparticles make favorable accomplishment of aqueous methyl orange (MO) and methylene blue (MB) dyes. Before the degradation reaction, two-step methods were executed to prepare nanocomposite (TiO₂/polyaniline) systems. Apart from synthesis, characteristics of the materials were perceived via x-ray diffraction, transmission electron microscopy, FOURIER transform infra red and UV-Vis techniques. The characteristic outcomes described the presence of polyaniline which suggestively impacts the size and crystallinity of TiO₂ and additionally, initiate π - π^* transition under visible light illumination. The π - π^* transition was excited to generate more electrons and holes in the nanocomposites and it helps to achieve visible light degradation of MO and MB.

Keywords: Metal oxide; Polyaniline; Conducting polymer; Methyl orange; Photocatalyst

1. Introduction

Pigments and synthetic dyes are regularly used for food, textile and cosmetic manufacturing units without appropriate management. Hence, these are straightly mixed into the body or water sources that cause numerous infections to every creature [1–3]. In this connection, nanomaterials were created a lot of impact for removing the contamination [1–12]. In the past four decades, titania (TiO₂) is comprehensively used as the finest catalyst for the exclusion of substantial organic metals from the industrial sewage via photocatalytic development under UV light condition [1,13]. Nowadays, the scientists are more likely to engage in the preparation of the visible light catalyst for the degradation process, because 41%–43% of visible light already exists in the solar spectrum [14,15]. However, still there is a big or major task for the researchers to elevate energetic materials for captivating visible light.

In the recent times, titania centralized nanocomposites such as TiO₂/semiconductors, TiO₂/metals and TiO₂/polymers

were extra eye-catching materials for the investigators caused by high efficiency for the degradation process and cost-effectiveness [14–18]. Exclusively, conjugated polymers incorporated TiO₂ show high degradation efficiency while compared with polymers based TiO₂. Because the conjugate polymers have high stability, capability to absorb visible light and generates more charge carriers [19–25]. Wang and Min [21] had stated that the effective degradation of methylene blue (MB) was attained with the use of TiO₂/polyaniline composites due to its high absorption capacity. The synergetic effect between polyaniline and TiO₂ is more favorable for the decomposition of gaseous acetone under UV and visible light [25]. On the other hand, Ansari et al. [23] had specified that the sensitizing outcome of polyaniline forms small bandgap of TiO₂ and their interfacial interaction has contributed high photocatalytic performance.

In this investigation, we have prepared different proportions of nanocomposite materials (TiO₂/polyaniline (1%, 3% and 5%)) by two-step method. To begin with sol-gel method was executed to prepare anatase TiO₂. Subsequently, oxidative-polymerization procedure was engaged to harvest

* Corresponding author.

the nanocomposite systems. Additionally, the belonging of nanocomposites was explored by transmission electron microscopy (TEM), x-ray diffraction (XRD), FOURIER transform infra red (FTIR) and UV. Besides, the synthesized systems were excellently employed as a catalyst for the degradation process under UV and visible light condition.

2. Experimental procedure

2.1. Materials

All the essential chemicals were obtained from Sigma-Aldrich (Pune). For pure TiO₂ preparation titanium tetraisopropoxide, cetyl trimethyl ammonium bromide, isopropyl alcohol and double distilled water are essential. Additionally, nanocomposite (TiO₂/polyaniline) has required diethylene glycol, aniline, ammonium peroxydisulfate, ethanol along with prepared TiO₂ powder. The photocatalytic testing has needed methyl orange (MO) and MB dyes. Further, all the aqueous solutions were prepared using double distilled water.

2.2. Preparation of pure TiO₂ and TiO₂/polyaniline systems

The synthesis steps of nanosized TiO₂ material were retained from our prior literatures [26–27]. In short, 1:5 ratio of titanium tetraisopropoxide and isopropyl alcohol was mixed along with 0.01 M of cetyl trimethyl ammonium bromide. The resultant white gel was calcined at 450°C for 1 h to attain pure anatase TiO₂ and then the material was labeled PT.

Preparation of TiO₂/polyaniline systems: at first, 0.5 M of ammonium peroxydisulfate was slowly added into aniline (0.1, 0.3 and 0.5 M) content. The above process helped to get polymerization via changing the monomer solution (aniline) into polymer (polyaniline). On the other side, 1 g of prepared TiO₂ powder was dissolved in 1 mol of diethylene glycol solution under constant stirring. Then, the above polymerized solution was mixed into the TiO₂ solution under continuous stirring overnight. After, the solution was filtered and washed several times with the use of ethanol. Finally, the gained powder was dried at 60°C for 3 h under vacuum oven. At the end, the nanocomposites were labeled TP1, TP3 and TP5 individually.

2.3. Photocatalytic testing

The photocatalytic reaction steps, source of light, preparation of dye, concentration of catalyst and dye were parallel to our previous reports. In short account, 100 mg of prepared materials (PT, TP1, TP3 and TP5) were taken separately. Then, the weighed catalyst was mixed into the 100 mL of aqueous MO and MB dye (5×10^{-5} mol/L). The above solutions were stirred continuously and irradiated with the use of UV (365 nm, 8W mercury lamp, Philips) and visible light (SF 300B, Sciencetech instrument with AM 1.5G cut-off filter). The absorption values before and after illuminated solution were monitored with the use of UV–Vis absorption spectrophotometer.

2.4. Characterization details

The X-ray D5000 diffractometer along with Cu K α 1 ($\lambda = 1.5406$ Å), Siemens instrument was performed to find

the degree of crystallinity. The shape and interface of the prepared materials were analyzed by Tecnai G2 200 kV, TEM. The RX1, PerkinElmer apparatus helped to determine the bandgap and absorption value of MO and MB dyes. A Rayleigh analytical FTIR tool (WQF-510A) was used to acquire the transmission spectra of the prepared materials.

3. Results and discussion

The purity, crystallinity and crystallite sizes of the synthesized PT and various proportions of nanocomposites (TP1, TP3 and TP5) were explored by XRD data. From Fig. 1(a), it is undoubtedly seen that the PT material has presented with fine crystalline nature. Moreover, the entire diffraction peaks were absolutely connected with anatase phase. The diffraction peaks spectacle without any combination of rutile and brookite phases which was well established by international centre for diffraction data. The confirmed anatase phase perfectly coincides with the JCPDS card number 89-4921 and their resultant crystallite size is 19.3 nm, which was calculated by Scherrer equation. Therefore, the above result obviously quantified that the synthesized material is in nanodimension. Fig. 1(b) shows pure polyaniline spectrum which expressed an amorphous nature. Later, the XRD patterns of the combination of polyaniline/TiO₂ materials are seen in Figs. 1(c)–(e). The consequences clearly denoted that the degree of crystallinity has reduced gradually with increasing polyaniline content [28]. Although, polyaniline content leads to change the crystalline nature of TiO₂, which infers that the prepared polyaniline is an amorphous nature. In the meantime, increasing the polyaniline content does not disturb the anatase phase aside from increase in peak width. The determined crystallite sizes of nanocomposites were 14.3, 11.9 and 8.2 nm for TP1, TP3 and TP5, respectively. This information demands that after the polymerization process, the polyaniline content suggestively impacts the size of TiO₂, because of synergistic effect which creates strong interface in-between polyaniline chain and TiO₂ nanoparticles [21–29].

The crystallinity and dimension of the synthesized PT, TP1, TP3 and TP5 were studied by TEM images. The exterior of the PT material (Fig. 2(a)) displays spherically fascinated

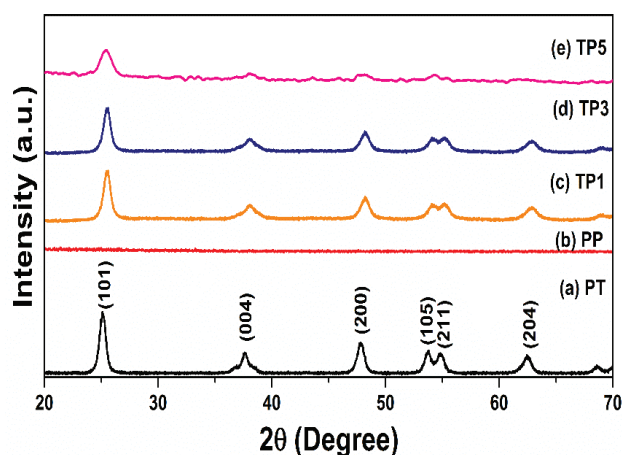


Fig. 1. XRD pattern of (a) PT, (b) PP, (c) TP1, (d) TP3 and (e) TP5.

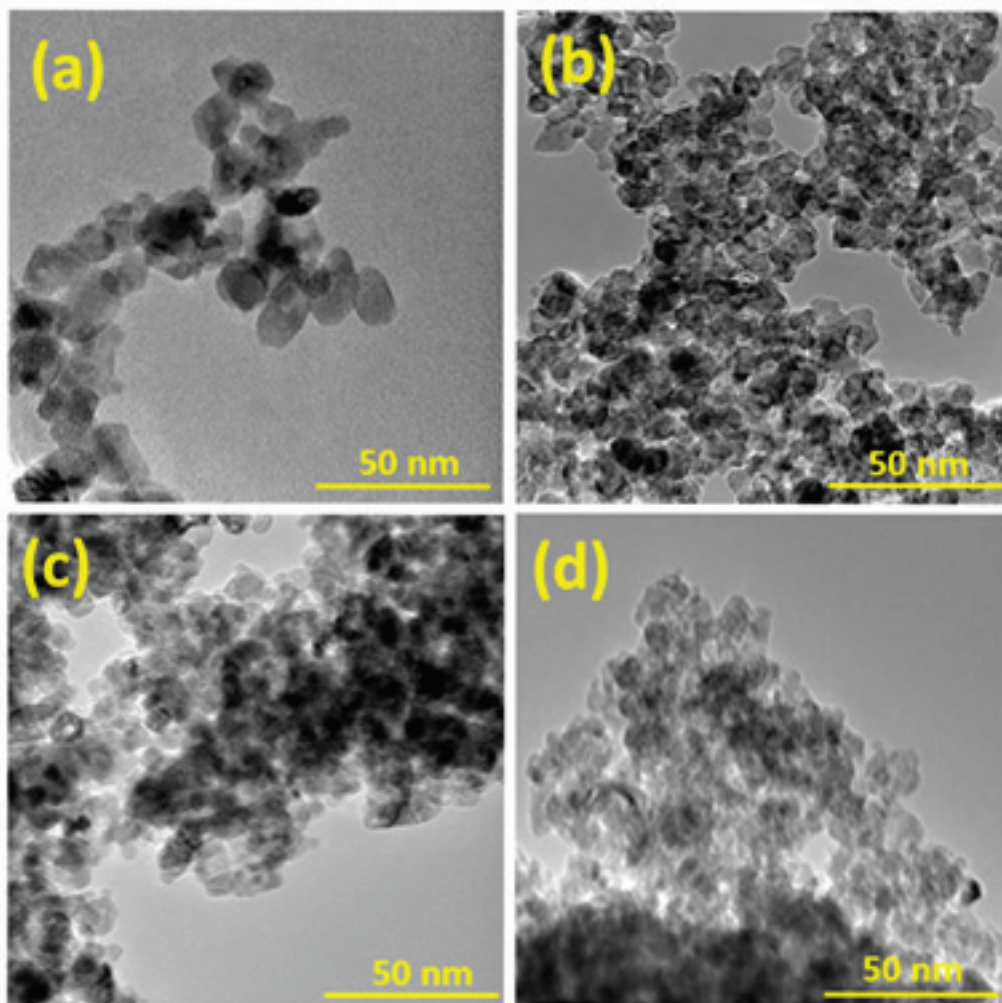


Fig. 2. TEM images of (a) PT, (b) TP1, (c) TP3 and (d) TP5.

particles in addition to fine crystalline nature and their average diameter is in-between 18 and 20 nm. Besides, TP1, TP3 and TP5 images (Figs. 2(b)–(d)) were curiously publicized that when the polyaniline content increases, the crystallinity of TiO_2 suggestively decreases with semicrystalline nature. Moreover, the fine nature of the particles was changed into agglomerated nature [29]. However, the polyaniline more interestingly increases the surface area via reducing the size (15, 12 and 8 nm for TP1, TP3 and TP5, respectively) because of synergetic interaction in-between polyaniline chain and TiO_2 particles [26–29].

The existing chemical bonds and its parallel functional groups were identified by FTIR measurement. The transmittance spectra of the synthesized systems (PT, TP1, TP3 and TP5) were scrutinized in-between 400 and 4,000 cm^{-1} . From Fig. 3(a), the stretching vibrations of PT material are spotted at 648, 1,409, 1,535 and 3,399 cm^{-1} which relates to Ti–O–Ti, C=O, Ti–OH and OH groups, respectively [21,27,30–33]. After the enclosure of polyaniline into TiO_2 , the materials were exhibited with the new stretching vibrations C–N, C=N, C=C and N–H along with Ti–O–Ti, C=O, Ti–OH and OH stretching modes. The above bonds are located at 1,153, 1,481, 1,550 and

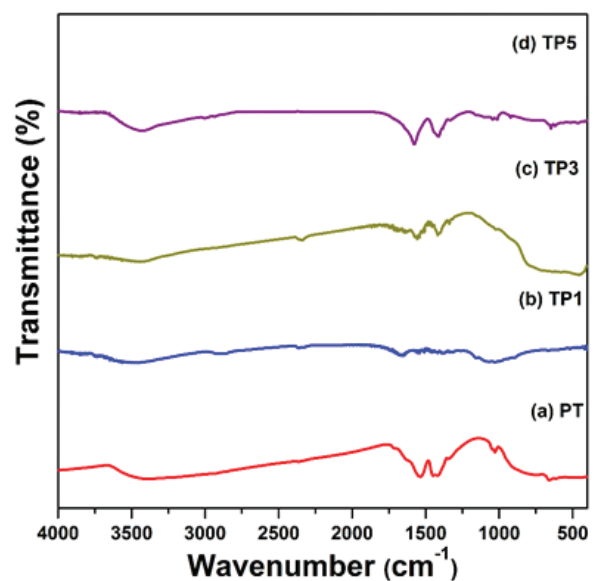


Fig. 3. FTIR spectra of (a) PT, (b) TP1, (c) TP3 and (d) TP5.

$3,210\text{ cm}^{-1}$. The above vibrations obviously quantified that the quinoid and benzenoid rings are obtainable in the TP1, TP3 and TP5 systems, which were originated from polyaniline content [21,24,30–33]. Hence, the FTIR outcomes unmistakably represent that those nanocomposite systems were comprised with the mixture of TiO_2 and polyaniline stretching vibrations.

The meticulous wavelength of the prepared (PT, TP1, TP3 and TP5) materials and its exact excitation transitions were explored via UV–Vis absorption spectrometer. In Fig. 4, the absorbance result for the PT material has revealed a solid transition arisen at 384 nm and their equivalent bandgap is determined as 3.25 eV. The above description recognized that the synthesized PT material has exposed a precise resilient absorption capability in the UV region. Later, the accumulation of polyaniline/ TiO_2 systems showed that the absorption wavelength has slightly moved to red-shift. The existence of polyaniline content has stimulated the polaron ($\pi\text{--}\pi^*$) transitions during the excitation [21,23,25,33].

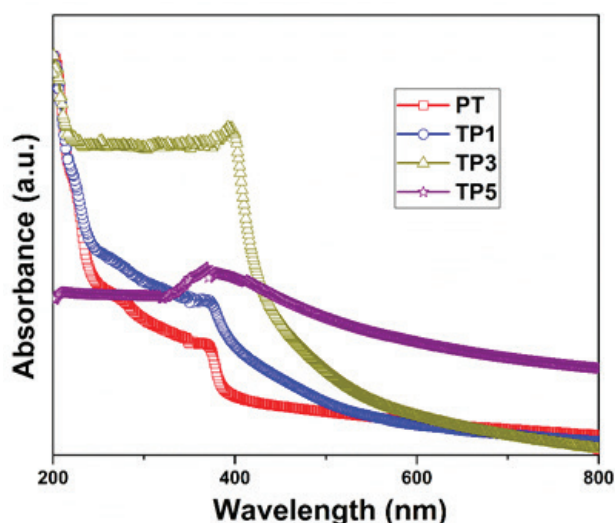


Fig. 4. UV–Vis absorbance spectra of (a) PT, (b) TP1, (c) TP3 and (d) TP5.

The FTIR outcomes have similarly established the presence of benzenoid and quinoid rings. Associated with other prepared materials, the absorption value of TP5 has broadened, because the higher amount of polyaniline leads to change the crystalline TiO_2 into semicrystalline or amorphous nature. Kang et al. [34] stated that the crystalline material has shown a strong sharp absorption band while related with amorphous material which was exposed with broad or wide absorption. Hence, the UV–Vis absorption consequences made clear that the prepared nanocomposites (TP1, TP3 and TP5) were actively participated during the visible light irradiation, because the absorption range is in the red region.

3.1. Photocatalytic degradation of MO and MB

The persistence of the current preparation is that the pure and nanocomposites (PT, TP1, TP3 and TP5) were competently used to destroy the organic dyes. In this report, the typical and more operational organic dyes (food, textile and cosmetic industries) such as MO and MB were carried as the model source for elimination process. The steadiness (stability) of the dyes was inspected under photoillumination at every 20 min exposed via UV (60 min) and visible light (180 min) and their consistent concentrations were monitored by UV–Vis spectrophotometer. The concentration values undoubtedly showed very slight changes (~ 0.05 negligible value). Under illumination, the concentration of dyes exhibited unaffected behavior, that is, the dyes showed more stability while excluding the catalyst. Afterwards, the above experiment was made identical with including the prepared catalyst into the MO or MB dye solution under UV and visible light illumination and their absorption wavelength was monitored at 464 and 664 nm respectively. Figs. 5(a) and (b) symbolize the C/C_0 value for the degradation of MO and MB with respect to time using the prepared catalyst and their reflection clearly displayed that the absorption value decreases with increasing irradiation time. After irradiation, the reliable degradation outcomes of the prepared materials were estimated, and their values are tabulated in Table 1.

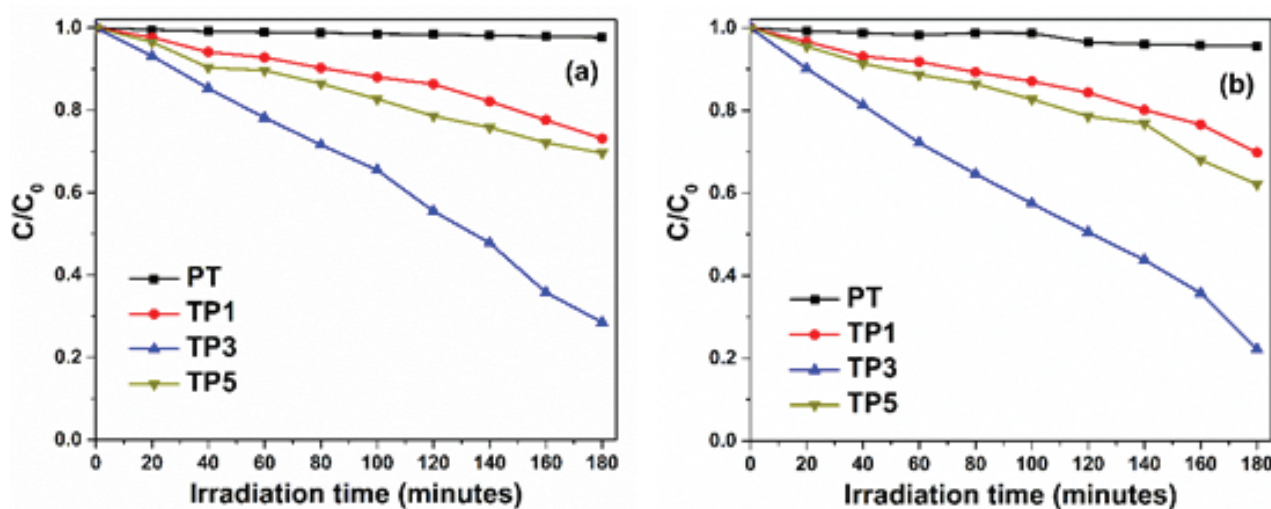


Fig. 5. The C/C_0 vs. visible irradiation time for the degradation of (a) MO and (b) MB dyes.

The outcome of degradation efficiencies stated that TP3 has superior activity due to its size and crystallinity [23,26–29]. Correlated with PT and TP1 characteristics, the size of TP3 is small that improves the surface property of the material which leads to attain high degradation [23,26–29]. On the other hand, good crystallinity and less agglomeration were detected from TP3 while compared with TP5.

The TP3 material has excellently removed the MO (86.9%) and MB (90.5%) solutions throughout the treatment of UV light (60 min) illumination. Additionally, under visible light condition, the material has expressed successful degradation of MO (71.5%) and MB (78.8%) solutions. Similarly, the prepared TP3 nanocomposite parades healthier results of degradations associated with other reports [21–25]. The MB has a simple structure and acts as a sensitizer which favors to attain higher degradation rate while compared with MO degradation [28,29]. Also, the TP3 material has displayed perfect recycling ability (Fig. 6) which suggests that the catalysts were used for long time durability. During UV light illumination, both TiO_2 and polyaniline actively produce more electrons and holes. Similarly, synergistic effect in-between TiO_2 and polyaniline postponed the recombination process. Therefore, the generated electrons–holes were aggressively participated to degrade MO and MB dyes via oxidation and reduction reactions [25,28].

The pathway diagram (Fig. 7) describes the visible light photocatalytic mechanism of nanocomposite system. During the irradiation process, polyaniline content has initiated π to π^* transition via excitation of the electrons from highest

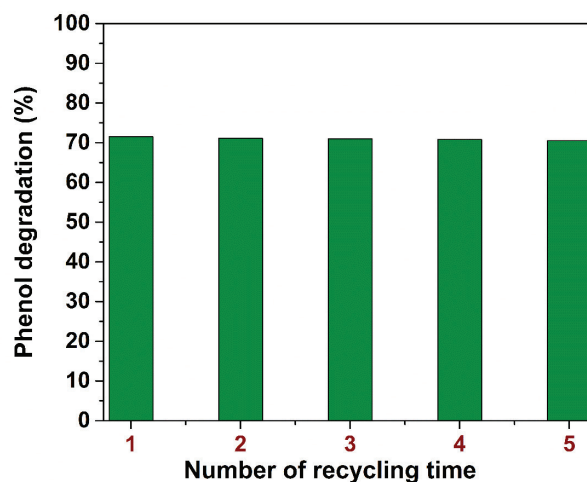


Fig. 6. The recycling process of TP3 material for the removal MO system.

Table 1

MO and MB degradation efficiency using synthesized pure and nanocomposites under UV and visible light irradiation

Materials	MO photodegradation – 60 min by UV light illumination (%)	MB photodegradation – 60 min by UV light illumination (%)	MO photodegradation – 180 min by visible light illumination (%)	MB photodegradation – 180 min by visible light illumination (%)
PT	65.3	72.4	2.3	4.5
TP1	68.9	75.9	27.9	31.2
TP3	86.9	90.5	71.5	78.8
TP5	70.3	78.4	30.4	37.9

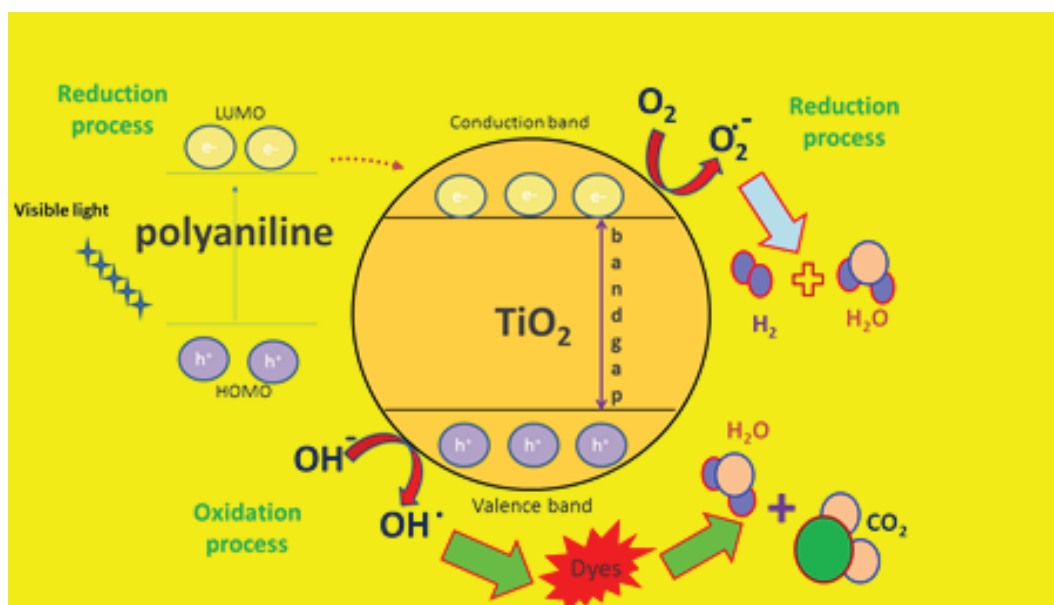


Fig. 7. The pathway diagram described visible light photocatalytic mechanism of nanocomposite (TiO_2 /polyaniline) system.

occupied molecular orbital (HOMO) to lowest unoccupied molecular orbital (LUMO). By this time, the HOMO state electrons stimulated the reduction reaction. Also, electrons are moved to the nearest energy level (conduction band of TiO_2). Mutually, the HOMO (polyaniline) and the conduction band (TiO_2) electrons were energetically participated in the reduction process. Simultaneously, the LUMO and valence band holes encouraged the oxidation process [21–25,28]. Therefore, the nanocomposite (TiO_2 /polyaniline) system has effectively participated to destroy the MO and MB dyes under visible light.

4. Conclusion

In this report, we had confirmed that while increasing the amount of polyaniline, there was a gradual decrease in crystallinity and size. Additionally, it creates bunch of agglomerated particles which was approved by XRD and TEM measurements. During visible light irradiation, the recognized $\pi-\pi^*$ transitions were ensured. This process had supported to generate more number of electrons and holes. Further, the presence of synergetic interactions had paved a way to obstruct the electrons–holes recombination. These processes helped the polyaniline/ TiO_2 materials magnificently to destroy MO and MB dyes.

Acknowledgment

We acknowledge Dr. K. Ravichandran, Departments of Nuclear Physics, University of Madras, India, for the lab facilities and his valuable contribution for the discussion.

References

- [1] C. Luo, X. Ren, Z. Dai, Y. Zhang, X. Qi, C. Pan, Present perspectives of advanced characterization techniques in TiO_2 -based photocatalysts, *ACS Appl. Mater. Interfaces*, 9 (2017) 23265–23286.
- [2] M.D. Hernández-Alonso, F. Fresno, S. Suárez, J.M. Coronado, Development of alternative photocatalysts to TiO_2 : challenges and opportunities, *Energy Environ. Sci.*, 2 (2009) 1231–1257.
- [3] K. Wenderich, G. Mul, Methods, mechanism, and applications of photo deposition in photocatalysis: a review, *Chem. Rev.*, 116 (2016) 14587–14619.
- [4] A.A. Alqadami, M. Naushad, M.A. Abdalla, M.R. Khan, Z.A. ALOthman, Adsorptive removal of toxic dye using Fe_3O_4 -TSC nanocomposite: equilibrium, kinetic, and thermodynamic studies, *J. Chem. Eng. Data*, 61 (2016) 3806–3813.
- [5] G. Sharma, M. Naushad, A. Kumar, S. Rana, S. Sharma, A. Bhatnagar, F.J. Stadler, A.A. Ghfar, M.R. Khan, Efficient removal of coomassie brilliant blue R-250 dye using starch/poly(alginic acid-clacrylamide) nanohydrogel, *Process Saf. Environ. Prot.*, 109 (2017) 301–310.
- [6] A.B. Albadarin, M.N. Collins, M. Naushad, S. Shirazian, Activated lignin–chitosan extruded blends for efficient adsorption of methylene blue, *Chem. Eng. J.*, 307 (2017) 264–272.
- [7] G. Sharma, A. Kumar, M. Naushad, A. Kumar, A.H. Al-Muhtaseb, P. Dhiman, A.A. Ghfar, F.J. Stadler, M.R. Khan, Photoremediation of toxic dye from aqueous environment using monometallic and bimetallic quantum dots based nanocomposites, *J. Cleaner Prod.*, 172 (2018) 2919–2930.
- [8] M. Thakur, G. Sharma, T. Ahamad, A.A. Ghfar, D. Pathania, M. Naushad, Efficient photocatalytic degradation of toxic dyes from aqueous environment using gelatin-Zr(IV) phosphate nanocomposite and its antimicrobial activity, *Colloids Surf., B*, 157 (2017) 456–463.
- [9] A.B. Albadarin, M. Charara, B.M.A. Tarboush, M.N.M. Ahmad, T.A. Kurniawan, M. Naushad, G.M. Walker, C. Magwand, Mechanism analysis of tartrazine biosorption onto masau stones; a low cost by-product from semi-arid regions, *J. Mol. Liq.*, 242 (2017) 478–483.
- [10] M. Naushad, Z.A. ALOthman, M. R. Awual, S.M. Alfadul, T. Ahamad, Adsorption of rose Bengal dye from aqueous solution by amberlite Ira-938 resin: kinetics, isotherms, and thermodynamic studies, *Desal. Wat. Treat.*, 57 (2016) 13527–13533.
- [11] D. Pathania, G. Sharma, A. Kumar, M. Naushad, S. Kalia, A. Sharma, Z.A. ALOthman, Combined sorptional–photocatalytic remediation of dyes by polyaniline Zr(IV) selenotungstophosphate nanocomposite, *Toxicol. Environ. Chem.*, 97 (2015) 526–537.
- [12] D. Pathania, R. Katwal, G. Sharma, M. Naushad, M.R. Khan, A.H. Al-Muhtaseb, Novel guar gum/ Al_2O_3 nanocomposite as an effective photocatalyst for the degradation of malachite green dye, *Int. J. Biol. Macromol.*, 87 (2016) 366–374.
- [13] R.E. Galian, J. Pérez-Prieto, Catalytic processes activated by light, *Energy Environ. Sci.*, 3 (2010) 1488–1498.
- [14] T.W. Kim, H.W. Ha, M.J. Paek, S.H. Hyun, J.H. Choy, S.J. Hwang, Unique phase transformation behavior and visible light photocatalytic activity of titanium oxide hybridized with copper oxide, *J. Mater. Chem.*, 20 (2010) 3238–3245.
- [15] S. Banerjee, S.C. Pillai, P. Falaras, K.E. O’Shea, J.A. Byrne, D.D. Dionysiou, New insights into the mechanism of visible light photocatalysis, *J. Phys. Chem. Lett.*, 5 (2014) 2543–2554.
- [16] R. Purbia, R. Borah, S. Paria, Carbon-doped mesoporous anatase TiO_2 multi-tubes nanostructures for highly improved visible light photocatalytic activity, *Inorg. Chem.*, 56 (2017) 10107–10116.
- [17] A.A. Nada, M. Nasr, R. Viter, P. Miele, S. Roualdes, M. Bechelany, Mesoporous $\text{ZnFe}_2\text{O}_4/\text{TiO}_2$ nanofibers prepared by electrospinning coupled to PECVD as highly performing photocatalytic materials, *J. Phys. Chem. C*, 121 (2017) 24669–24677.
- [18] H. Wei, W.A. McMaster, J.Z.Y. Tan, L. Cao, D. Chen, R.A. Caruso, Mesoporous $\text{TiO}_2/\text{g-C}_3\text{N}_4$ microspheres with enhanced visible-light photocatalytic activity, *J. Phys. Chem. C*, 121 (2017) 22114–22122.
- [19] B. Muktha, G. Madras, T.N.G. Row, U. Scherf, S. Patil, Conjugated polymers for photocatalysis, *J. Phys. Chem. B*, 111 (2007) 7994–7998.
- [20] J. Park, Visible and near infrared light active photocatalysis based on conjugated polymers, *J. Ind. Eng. Chem.*, 51 (2017) 27–43.
- [21] F. Wang, S.X. Min, TiO_2 /polyaniline composites: an efficient photocatalyst for the degradation of methylene blue under natural light, *Chin. Chem. Lett.*, 18 (2007) 1273–1277.
- [22] Y. Lin, D. Li, J. Hu, G. Xiao, J. Wang, W. Li, X. Fu, Highly efficient photocatalytic degradation of organic pollutants by PANI-modified TiO_2 composite, *J. Phys. Chem. C*, 116 (2012) 5764–5772.
- [23] M.O. Ansari, M.M. Khan, S.A. Ansari, M.H. Cho, Electrically conductive polyaniline sensitized defective- TiO_2 for improved visible light photocatalytic and photoelectrochemical performance: a synergistic effect, *New J. Chem.*, 39 (2015) 8381–8388.
- [24] N. Wang, J. Li, W. Lv, J. Feng, W. Yan, Synthesis of polyaniline/ TiO_2 composite with excellent adsorption performance on acid red G, *RSC Adv.*, 5 (2015) 21132–21141.
- [25] J. Wei, Q. Zhang, Y. Liu, R. Xiong, C. Pan, J. Shi, Synthesis and photocatalytic activity of polyaniline- TiO_2 composites with bionic nanopapilla structure, *J. Nanopart. Res.*, 13 (2011) 3157–3165.
- [26] L. Gnanasekaran, R. Hemamalini, K. Ravichandran, Synthesis and characterization of TiO_2 quantum dots for photocatalytic application, *J. Saudi Chem. Soc.*, 19 (2015) 589–594.
- [27] L. Gnanasekaran, R. Hemamalini, R. Saravanan, K. Ravichandran, F. Gracia, V.K. Gupta, Intermediate state created by dopant ions (Mn, Co and Zr) into TiO_2 nanoparticles for degradation of dyes under visible light, *J. Mol. Liq.*, 223 (2016) 652–659.

- [28] R. Saravanan, E. Sacari, F. Gracia, M.M. Khan, E. Mosquera, V.K. Gupta, Conducting PANI stimulated ZnO system for visible light photocatalytic degradation of coloured dyes, *J. Mol. Liq.*, 221 (2016) 1029–1033.
- [29] V.K. Gupta, R. Saravanan, S. Agarwal, F. Gracia, M.M. Khan, J. Qin, R.V. Mangalaraja, Degradation of azo dyes under different wavelengths of UV light with chitosan-SnO₂ nanocomposites, *J. Mol. Liq.*, 232 (2017) 423–430.
- [30] B. Ozbay, N. Genc, I. Ozbay, B. Baghaki, S. Zor, Photocatalytic activities of polyaniline-modified TiO₂ and ZnO under visible light: an experimental and modeling study, *Clean Technol. Environ. Policy*, 18 (2016) 2591–2601.
- [31] N. Parveen, M.O. Ansari, M.H. Cho, Route to high surface area, mesoporosity of polyaniline–titanium dioxide nanocomposites via one pot synthesis for energy storage applications, *Ind. Eng. Chem. Res.*, 55 (2016) 116–124.
- [32] J. Zhu, X. Huo, X. Liu, H. Ju, Gold nanoparticles deposited polyaniline–TiO₂ nanotube for surface plasmon resonance enhanced photoelectrochemical biosensing, *ACS Appl. Mater. Interfaces*, 8 (2016) 341–349.
- [33] A.M. Youssef, Morphological studies of polyaniline nanocomposite based mesostructured TiO₂ nanowires as conductive packaging materials, *RSC Adv.*, 4 (2014) 6811–6820.
- [34] Y. Kang, Y. Yang, L.C. Yin, X. Kang, G. Liu, H.M. Cheng, An amorphous carbon nitride photocatalyst with greatly extended visible-light-responsive range for photocatalytic hydrogen generation, *Adv. Mater.*, 27 (2015) 4572–4577.